Desalination and Water Treatment
www.deswater.com
doi: 10.1080/19443994.2015.1096830

57 (2016) 19160–19170
September

Taylor & Francis
Taylor & Francis Group

Genetic programming for modeling and optimization of gas sparging assisted microfiltration of oil-in-water emulsion

Akbar Asadi Tashvigh, Farzin Zokaee Ashtiani*, Amir Fouladitajar

Department of Chemical Engineering, Amirkabir University of Technology, No. 424, Hafez Ave., Tehran, Iran, Tel. +98 9358748465; email: akbar.asadi@aut.ac.ir (A. Asadi Tashvigh), Tel. +98 21 6454 3124; Fax: +98 21 66405847; email: zokaee@aut.ac.ir (F. Zokaee Ashtiani), Tel. +98 9124990549; email: fouladi@aut.ac.ir (A. Fouladitajar)

Received 14 February 2015; Accepted 11 September 2015

ABSTRACT

Genetic programming (GP) is an orderly method based on natural evolution rules for getting computers to regularly solve a problem. In the present study, GP is presented as a novel approach for modeling the gas sparging assisted microfiltration of oil-in-water emulsion process. The effects of gas flow rate (Q_G), oil concentration (C_{oil}), transmembrane pressure (TMP), and liquid flow rate (Q_L) on the permeate flux and oil rejection were studied and the GP models were developed to predict the membrane performance. C_{oil} and TMP showed significant effects on both permeate flux and rejection. An interaction between C_{oil} and TMP was detected, at low C_{oil} and high TMP, in which the permeate flux increased considerably. It was found that Q_L has a low effect on permeate flux, but its impact on rejection was significant. Increasing Q_L from 0.5 to 2.75 L/min led to a considerable increment in rejection; however, further increase in the liquid flow rate decreased the oil rejection. On the contrary, Q_G showed a small effect on oil rejection, but its effect on permeate flux was notable. To determine the optimum conditions, the performance index was maximized using the developed genetic algorithm. Under the obtained optimal conditions, maximum permeate flux and rejection (%) were 121.6 (Lm^2/h) and 93.0%, respectively.

Keywords: Oil-in-water emulsion; Microfiltration; Gas sparging; Genetic programming; Optimization

1. Introduction

Nowadays, a large volume of wastewater produced from various industries such as oil, gas, petrochemical, food, transportation, and metallurgical industries is discharged into the environment which mostly contains oil-in-water emulsions [1,2]. It has been shown in the recent decade that membrane technology can be successfully used to treat these kinds of wastewaters [3,4]; however, fouling and concentration polarization have still remained as disadvantages of these processes which should be overcome [5–7]. Different studies have been done to reduce fouling and improve membrane performance including module design, manipulating fluid flow hydrodynamics, shear increase devices, improving membrane material and hydrophobicity [8–13], gas sparging [14,15], etc. Application of gas–liquid two-phase flow to enhance permeate flux, particularly for MF and UF processes, has been proven to be an efficient technique [16]. The use of gas bubbling in membrane processes was

*Corresponding author.

reviewed by Cui et al. [14], and it is reported that the gas sparging method may destroy the concentration polarization layer thickness and increase the permeate flux in most cases [16]. Many other works have been done in recent years which have been extensively reviewed in previous work [16].

Making reliable models to study industrial processes is a useful tool which helps to control and optimize the processes [17–19]. Mathematical modeling of any process is possible by two different approaches: (1) theoretical models that comprise basic principles of processes and (2) empirical models that do not need any knowledge of process and governing principles [20].

The preference of empirical models over the theoretical models consists of the possibility to develop rapidly the response function useful for process optimization [17]. Genetic programming (GP) as a branch of genetic algorithm (GA) has proved to be a powerful tool capable of modeling highly complex and nonlinear systems in a wide variety of applications such as engineering, medical, etc. [21–25]. Although GP is a progressive technique for commonly generating nonlinear input–output empirical models (mathematical expression) in any complex system, its application in predicting membrane processes is limited.

Okhovat and Mousavi [26] used GP to model nanofiltration (NF) process. They applied GP for prediction of the membrane rejection of arsenic, chromium, and cadmium ions in a NF pilot-scale system with regards to the feed concentration and transmembrane pressure (TMP) as input parameters. The results showed quite satisfactory accuracies of the proposed models and nominated GP as a potential tool for identifying the behavior of a membrane process. Suh et al. [27] investigated the application of GP to construct a model for prediction of membrane damage in the membrane integrity test. They employed GP as a novel approach to develop a model to predict the area of membrane breach with other experimental conditions (concentration of fluorescent nanoparticle, the permeate water flux, and TMP). The developed GP showed high capability of prediction of the area of the membrane breach and, with the simple membrane integrity test, the GP technique provided a practical way for estimating the degree of membrane damage.

In previous work [28], treatment of oil-in-water emulsion was experimentally investigated in a gas sparging assisted MF process and a quadratic model were proposed by response surface methodology (RSM) to predict permeate flux and oil rejection. Although the results were satisfactory, GP was used in the current work to model the same process to obtain easier and more accurate model for gas-sparged MF processes. Four different operating parameters (including gas and liquid flow rates, oil concentration, and TMP) were considered as the input variables of GP. The model accuracy was then checked and validated by the obtained experimental data and discussed in detail.

2. Genetic programming

GP was introduced by Koza [29] for the first time as a method to genetically develop mathematical relations for prediction of a system behavior with even high complexity. GP, which is based on the bio-inspired technique, defined as an automatically defined function that is able to automatically discover a computer program that predicts a system or problem well [22]. Every program in the GP is expressed as a tree function. An example of a GP tree is illustrated in Fig. 1. The binary arithmetic functions, "−", "+", and "*" each have two sub-trees. The sub-tree on the right containing "*", "y", and "z", represents the mathematical expression "$y * z$". The tree as a whole represents $f(w, x, y, z) = y * z + w - \cos(x)$. In Fig. 1, the connections points are known as nodes. With regard to the position in GP tree, these nodes are divided into two types as:(1) Internal nodes are called as function (nonterminal); these function nodes use one or more input values and generate a single output value (e.g. +, −, ×, sin, cos, exp, etc.) and provide the internal cells with expression trees; (2) nodes at the end of trees (leaf nodes) are called terminal and indicate input variables and zero augments.

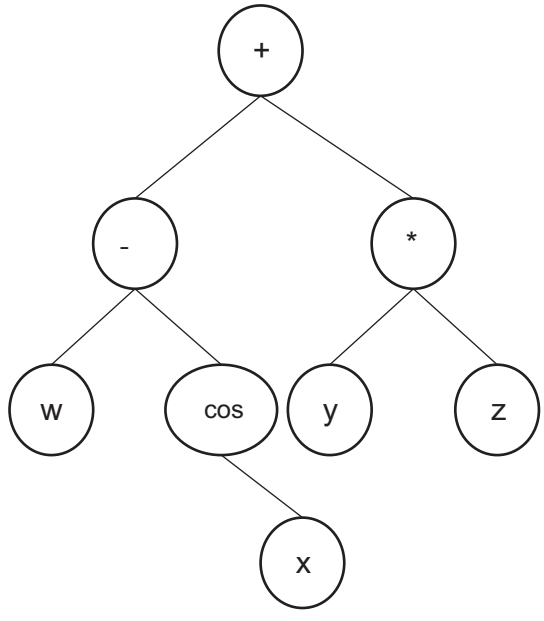

Fig. 1. Sample of a GP tree.

Fig. 2 is a flowchart of a GP modeling procedure. The basic mechanism of GP for a specific problem that requires finding a mathematical model is based on a repetitive computational process. Based on the procedure shown in Fig. 2, once the problem data is loaded, the initial population of programs is created randomly. In the next step, fitness value, which quantifies how well the program solves the problem, for the population evaluates. New generations of programs are iteratively created by selecting parents based on their fitness and breeding them via genetic operators including crossover, mutation, and reproduction.

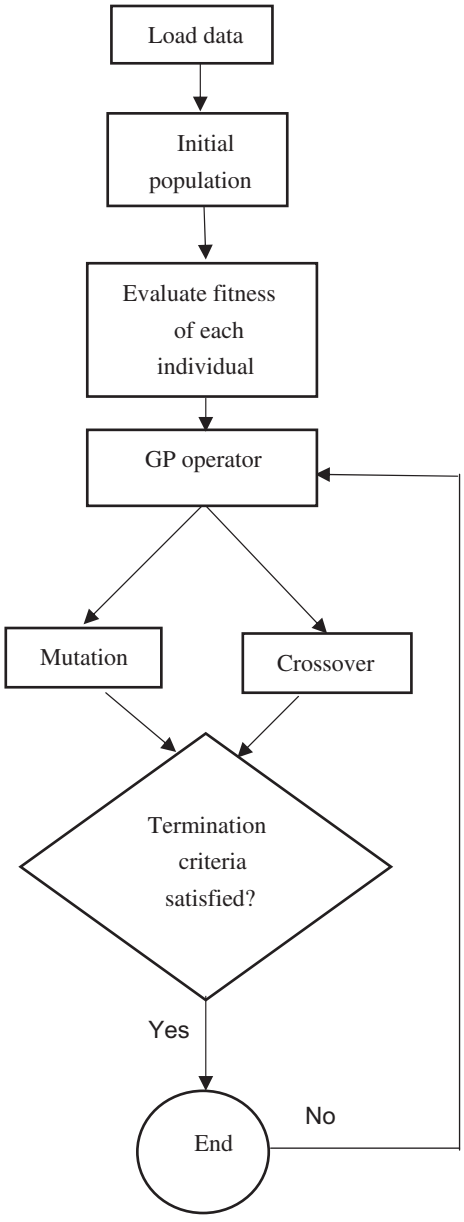

Fig. 2. GP problem solving approach procedure.

According to selecting better individuals and passing their best characteristics to their offspring, the population tends to improve in quality along successive generations. This evolutionary process continues until a termination criterion (maximum number of generation) is verified. Detailed descriptions of the GP procedure are provided in our previous work [21]. This study uses the GP method to find a mathematical expression for prediction of permeate flux and oil rejection of gas sparging assisted MF process. The terminals are set as [Q_G, C_{oil}, TMP, and Q_L], and the functions are set as [+, −, *, /, sin, cos, tanh], and the fitness function evaluates the root mean square error (RMSE) between the value from original learning data-set and that of each chromosome.

3. Experimental

3.1. Feed preparation and membrane

The oil-in-water emulsion was prepared by mixing gas oil and surfactant in distilled water at a mixing rate of 12,000 rpm for 30 min. The surfactant was used at a concentration of 100 mg/L. A brief description about feed and membrane properties is presented in Table 1.

3.2. Experimental setup

The stable emulsion feed was held in a 10-L tank. A centrifugal recirculation pump controlled by an inverter was used to deliver the feed to the membrane module and also provided the required constant operating pressure of the oil-in-water emulsion. A flow meter, calibrated for the present experiments, was utilized. The required air flow was supplied by a 25-L compressor with adjustable gas velocity, equipped with both regulator and flow meter. Gas and liquid were mixed just before entering the module. Permeate was collected and regularly returned to the storage tank to guarantee a constant feed concentration. The system was able to adjust and control the important operating parameters, including operating pressure, and liquid and gas velocity. The membrane module was specifically designed and fabricated from Plexiglas to observe gas–liquid two-phase flow regimes, Fig. 3. A brief limitation of model variables are reported in Table 2. More details about the module and the experimental procedure have been given in previous work [16].

Depending on gas and liquid velocities, four distinct flow patterns, from bubbling to churn flow, were observed in the flat-sheet microfiltration module, shown in Fig. 4. Sparse bubbles were observed at low gas velocities which formed a dense uniform bubble

Table 1
Physical properties of the feed and membrane

Feed Properties	
Oil type	Gas oil
Oil density at 15℃	845 kg/m^3
Kinematic viscosity of oil at 37.8℃	3.8 cSt
Surfactant	Polyoxyethylene (80) Sorbitan Monooleate (Tween 80, Merck)
Membrane Properties	
Material	(PVDF, Millipore Co.)
Mean pore size	0.45 μm
Thickness	125 μm
Porosity	70%
Effective membrane area	50 cm^2

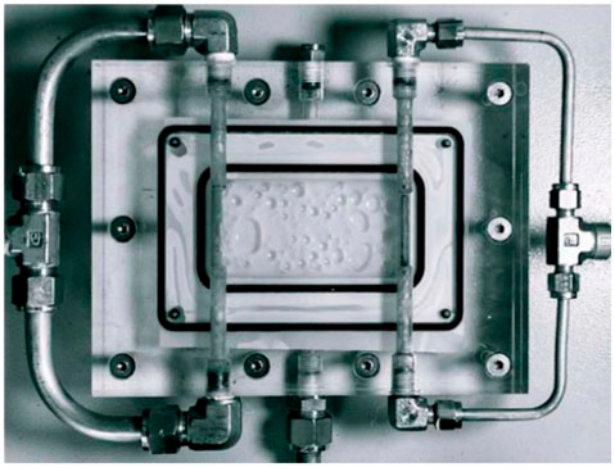

Fig. 3. Membrane module.

Table 2
Limitation of variables used for GP models construction

Variables	Range
Input variables	
Q_G (L/min)	0.2–2.1
Q_L (L/min)	0.8–3.2
Reynolds Number	125–1,350
C_{oil} (mg/L)	100–10,900
TMP (bar)	0.9–2.1
Ratio of Q_G/Q_L	0.8–2
Output variables	
Flux (Lm^2/h)	42–174.22
Rejection (%)	66.4–95.1

flow as the gas velocity increased, Fig. 4(a) and (b). Then, slug flow pattern appeared at intermediate gas velocities, Fig. 4(c). Churn flow regime was observed at higher gas velocities (Q_G = 2 L/min), Fig. 4(d). At higher gas velocities, the gas flow became dominant which resulted in annular flow being undesirable.

4. Results and discussion

4.1. Permeate flux and oil rejection modeling

Experimental data from previous work [28] were used in order to investigate the effect of gas flow rate ranging from 0.2 to 2.1 L/min, feed concentration, (100–10,900 mg/L), TMP (0.9, 1, 1.5, 2, and 2.1 bar), and feed flow rate ranging from 0.8 to 3.2 L/min on the permeate flux and rejection of oil. For more descriptions about experimental part, readers are referred to previous work [28]. The data used for GP modeling can be seen in Appendix 1. 90% of all the experimental data were used for training and validation of the model and the remaining were used as the test data. The performance of finding a good estimation model with low error was not improved over 250 generations and 200 populations. The optimum tree depth was 6. The fitness function evaluates RMSE of each individual among the experimental values and that is returned by the individual. The best GP models obtained after satisfying the termination criteria are:

$$y_1 = 3.01x_4 + 38.28\cos(\cos(x_2)) - 2106.0\cos(\sin(x_3)) + 41.56\tanh(\exp(x_1)) + 38.28\sin(\sin(x_1)) + 17.33\tanh(x_3 - 0.629\exp(\sin(x_1)) + \sin(\sin(\sin(x_2)))) + 251.4\sin(3.084x_1) - 41.56\sin(\sin(\sin(x_2))) - 0.0028x_3(x_2 - x_4 + \tanh(x_1 + x_3)*(x_2 + x_3 - x_4 - \sin(x_1) + \sin(x_2) - 3.051)) + 1407.0 \quad (1)$$

$$y_2 = 0.001696\,x_2 - 22.54\,x_3 - 0.001696\tanh(\exp(x_3)(x_1 + x_2)) + 726.1\,\exp(\sin(\tanh(\exp(x_3)))) + 5.027\exp(\tanh(\cos(x_2x_3))) - 0.001696\,\cos(\cos(x_3) - \sin(x_3)) - 1.6\,\sin(\exp(x_4) - \cos(2x_2) - x_4 - \tanh(x_1^2(x_1 + x_4)) + 7.195) + 0.04065\,x_1(x_1 + 7.625) + 3.091\sin(\sin(x_3 - 7.452))\tanh(\tanh(x_3 - x_4)) + 0.01498\,x_1\exp(x_1) + 3.052\,x_3\sin(x_2) - 1582.0 \quad (2)$$

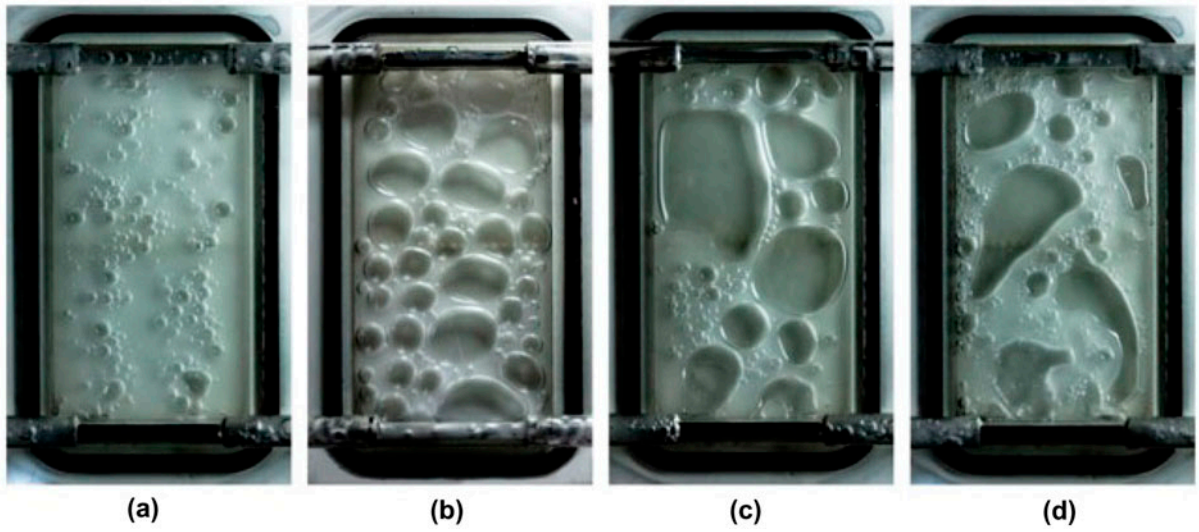

Fig. 4. Gas–liquid two-phase flow patterns in the flat-sheet microfiltration module for Q_L = 1 L/min and different gas flow rates: (a) sparse bubble Q_G = 0.25 L/min, (b) dense bubble Q_G = 0.5 L/min, (c) slug Q_G = 0.75 L/min and (d) churn flow Q_G = 2 L/min.

where x_1, x_2, x_3, and x_4 denote the Q_G, C_{oil}, TMP, and Q_L, respectively, y_1 and y_2 are the permeate flux and oil rejection, respectively.

The performance of GP models is illustrated in Figs. 5 and 6. The predicted permeate flux and oil rejection are plotted vs. experimental results for training data in Fig. 5(a) and (b). Fig. 6(a) and (b) shows the GP model results for the test data. As shown in this figure, GP model provided good agreement between experimental and predicted data for both permeate flux and oil rejection. Obtained R^2 are 0.945 and 0.981 for permeate flux and oil rejection, respectively. As it can be seen from Figs. 5 and 6, the GP models successfully predicted the process performance with a great agreement to the experimental data. Also, as shown in Figs. 5(b) and 6(b), GP performance for test data (those which were not used for model development) was evaluated in the range of data which was used for construction of models. Therefore, it should be noted that, GP modeling results are well for prediction of system behavior in the range of operating condition used for model training. Although GP has been used for extrapolation with an acceptable error in some previous studies [30], in the present study there was no need for extrapolation, and approximately, the whole range of operating condition for MF process was considered experimentally.

In order to investigate the reliability of the developed GP models, some statistical analyses were done and the results are given in Table 3. The results show that the developed models are significant and the predicted data are in great agreement with the experimental ones. The "R^2" value of near to unity for the presented GP models showed that the results are fitted to the experimental data very well. Other statistical

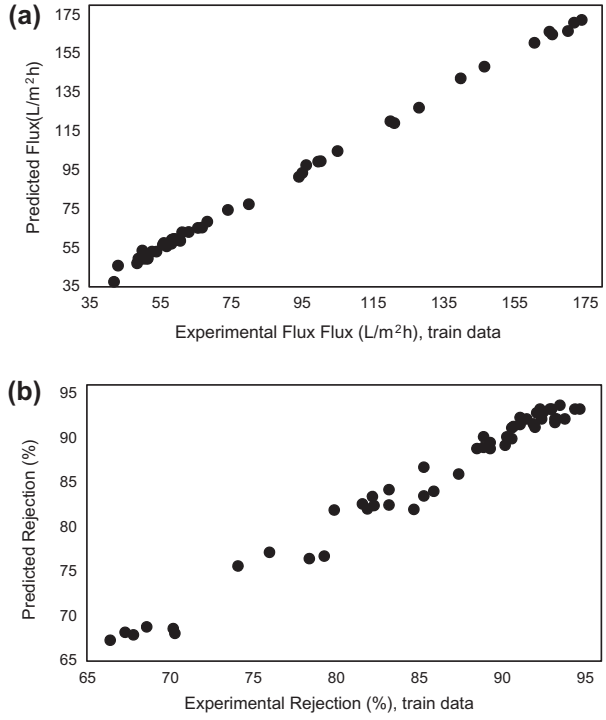

Fig. 5. GP performance for training data (a) permeate flux and (b) oil rejection.

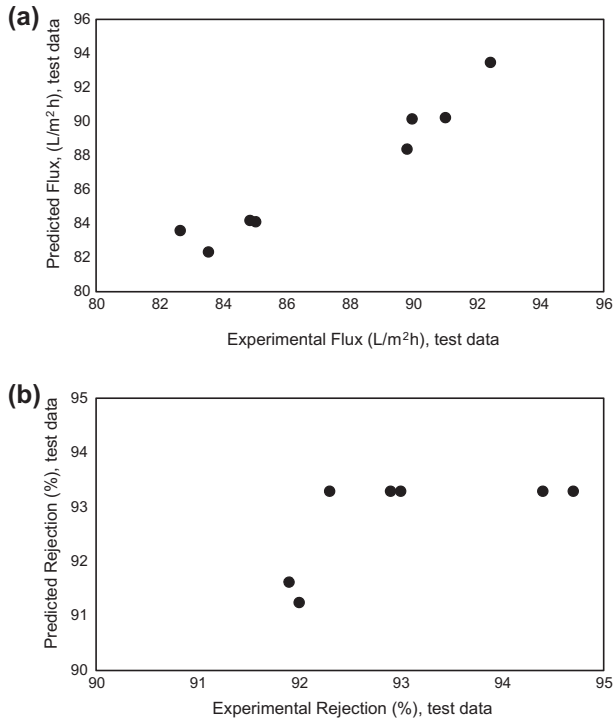

Fig. 6. GP applicability for test data (a) permeate flux and (b) oil rejection.

parameter values also showed that it has some insignificant errors in the prediction of the experimental results. In addition, the analysis of variance (ANOVA) has been employed for test data in order to validate statistically the constructed GP models and the ANOVA results are summarized in Table 4. According to this statistical test, the *F*-values (ratio of variances) are quite high (3,560.8 and 40,339.67) and the *p*-values (probability value in statistical significance testing) are smaller than 0.0001 which confirm the model validity. All these statistical estimators reveal that the constructed GP models are statistically valid for the prediction of the responses in the region of experimentation.

4.2. Effects of operating parameters

The developed GP model was applied to plot 2D diagrams showing the interaction of two variables on the permeate flux and oil rejection.

Fig. 7(a) shows the influence of the gas flow rate (Q_G) and the feed flow rate (Q_L) on the permeate flux. As can be seen from Fig. 7(a), increasing Q_G leads to an enhancement of permeate flux, whereas the influence of Q_L on permeate flux is insignificant. The effects of Q_G and Q_L on the oil rejection have also been illustrated in Fig. 7(b). As shown in Fig. 7(b), Q_G has little effect on the oil rejection, and increasing the Q_L until 2.75 L/min leads to increase in oil rejection and furthermore increment in Q_L leads to decrease in oil rejection.

Fig. 8(a) shows the effects of the feed concentration (C_{oil}) and TMP on the permeate flux. As it was expected, on decreasing the C_{oil} and increasing the TMP, permeate flux tends to increase. An interaction effect between C_{oil} and TMP was detected. For example, at low values of C_{oil} and a high value of TMP, permeate flux increases considerably due to the synergetic effect between these two input variables. The influence of C_{oil} and TMP on the oil rejection has been illustrated in Fig. 8(b). The feed concentration has a direct effect on the oil rejection, as feed concentration increases, oil rejection increases, but TMP has an inverse effect, as TMP increases, oil rejection tends to decrease.

4.3. Process optimization

The optimization should be done based on the performance index (the oil rejection factor times the permeate flux) as done by Khayet and Cojocaru [31]. Therefore, the constructed GP models have been used to optimize the gas sparging assisted MF process. GA was employed for optimization. The computed optimum conditions given by the GP models are summarized in Table 5. It is shown that the GP results are more accurate than those obtained by RSM reported in previous work [28].

4.4. Parameter analysis

As mentioned in Section 4.1, the effect of operating condition on the permeate flux and oil rejection was considered for modeling. It is also important to

Table 3
Statistical parameters for training and test data

Statistical parameter	R^2		SSE		MSE		RMSE		NB%	
	PR	OR	PF	OR	PF	OR	PF	OR	PF	OR
Training data	0.999	0.98	124.21	67.374	2.484	1.367	1.576	1.169	−0.004	−0.001
Test data	0.945	0.981	7.361	14.255	0.92	1.782	0.959	1.335	−0.004	0.001

Table 4
ANOVA of the test data

Source	DF[a]		SS[b]		MS[c]		*F*-value		*p*-value	
	Permeate Flux	Oil rejection	Permeate Flux	Oil rejection	Permeate Flux	Oil rejection	Permeate Flux	Oil rejection	Permeate Flux	Oil rejection
Model	1	1	30,561.16	34,161.34	30,561.16	34,161.34	35,60.8	40,339.67	<0.0001	<0.0001
Residual	14	14	120.15	11.85	8.58	0.84				
Total	15	15	30,681.32	34,173.2						

Notes: [a]Degree of freedom.
[b]Sum of squares.
[c]Mean square.

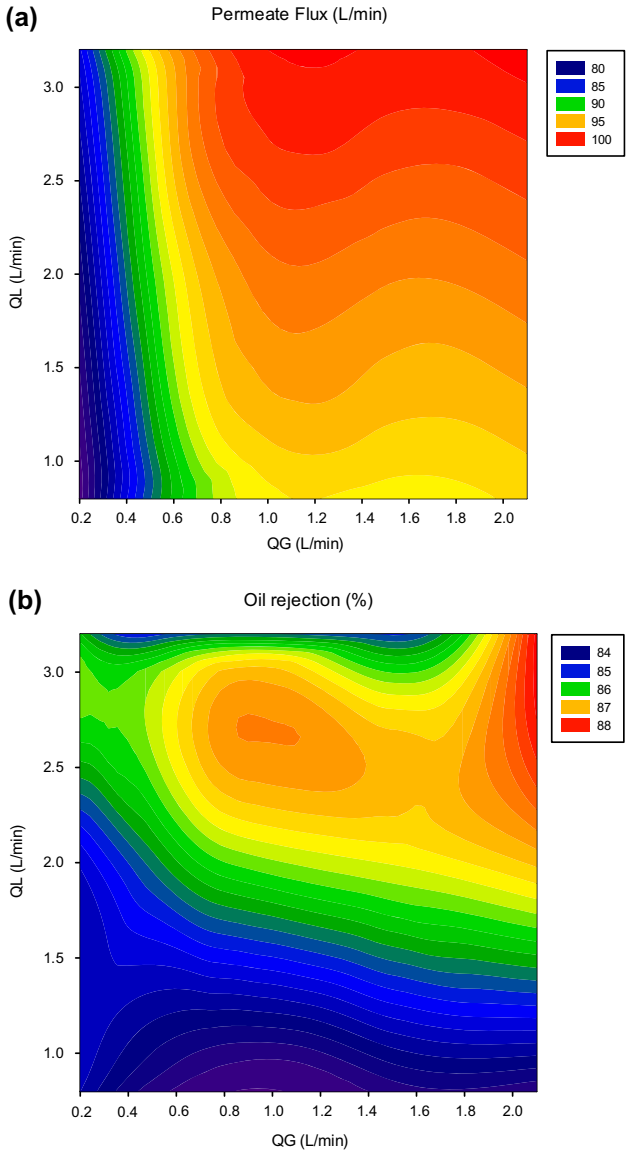

Fig. 7. The effects of Q_G and Q_L on the gas sparging assisted MF process performance for C_{oil} = 1,000 mg/ L and TMP = 1 bar (a) permeate flux and (b) oil rejection.

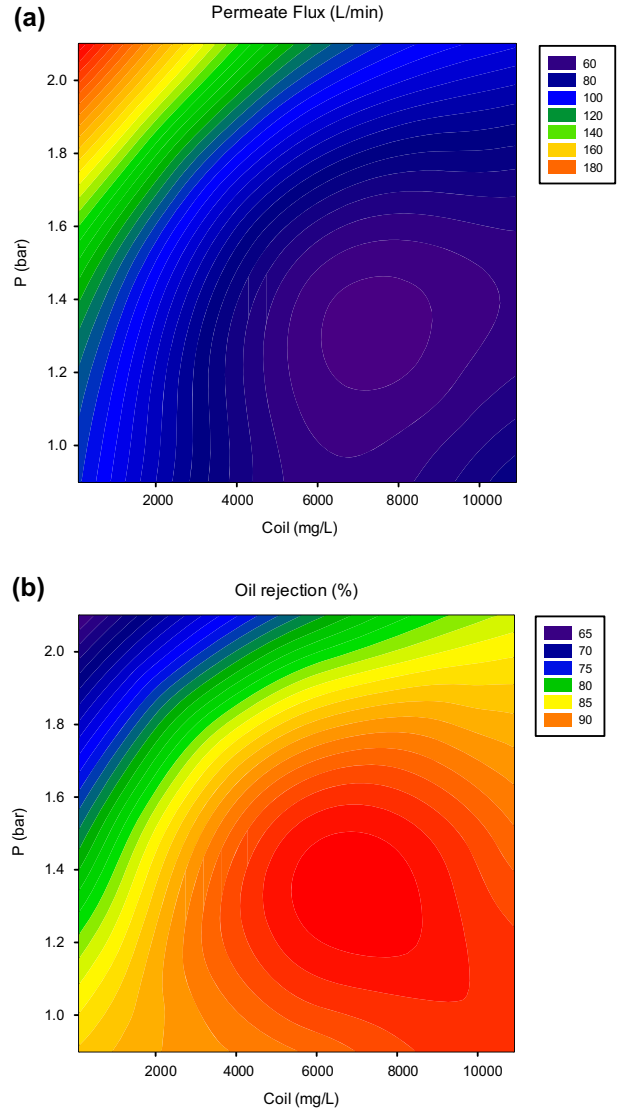

Fig. 8. The effects of C_{oil} and TMP on the gas sparging assisted MF process performance for Q_G = 1.5 L/min and Q_L = 2 L/min (a) permeate flux and (b) oil rejection.

know significant parameters. Since constructed GP models are mathematical expressions, its derivative can be calculated simply, to this end, derivative of process performance function; Eq. (1) times Eq. (2), in the optimum point is calculated and reported in Table 6. As it is seen, TMP is the most significant parameter and oil concentration has an intermediate effect on the process performance. Other remaining factors have an equal importance, approximately. This type of analysis is useful to economically process optimization.

Table 5
Optimal value for gas sparging assisted MF process

Q_G (L/min)	C_{oil} (mg/L)	TMP (bar)	Q_L (L/min)	Flux (L/min)	Rejection (%)
1.73	5,860.64	1.102	2.96	121.59	93.02

Table 6
Percentage of importance of operating parameters on the process performance

Q_G	C_{oil}	P	Q_L
12.26	18.50	58.29	10.95

5. Conclusions

An important objective of this work was to obtain a GP model to predict the membrane performance in a gas sparging assisted microfiltration of oil-in-water emulsion process. The effects of operating parameters including gas and liquid flow rates, oil concentration and TMP on the permeate flux and oil rejection (%) were studied. It was shown that the developed GP model was able to predict the process with an excellent accuracy. The most significant and effective parameters on the permeate flux were found to be oil concentration, Q_G and TMP. Also there were some interactions between the following input variables: (i) interaction between oil concentration (C_{oil}) and TMP in permeate flux and oil rejection; (ii) moderate interaction between gas flow rate (Q_G) and liquid flow rate (Q_L) in oil rejection. Based on the developed GP models, the process performance index was optimized using GA method. The obtained optimal solution represents the best process operating conditions (Q_G = 1.73 L/min, C_{oil} = 5,860.6 mg/L, TMP = 1.10 bar, Q_L = 2.96 L/min) with a maximum performance index (11,310.69 Lm^2/h), in which the permeate flux and oil rejection were found to be 121.59 Lm^2/h and 93.0%, respectively. Obtained optimal condition using GP model showed 20% increase in process performance in comparison to the obtained results from RSM in previous work [16], also the accuracy of the present model is higher than response surface method.

References

[1] M. Abbasi, M.R. Sebzari, A. Salahi, S. Abbasi, T. Mohammadi, Flux decline and membrane fouling in cross-flow microfiltration of oil-in-water emulsions, Desalin. Water Treat. 28 (2011) 1–7.

[2] A. Asadi Tashvigh, A. Fouladitajar, F. Zokaee Ashtiani, Modeling concentration polarization in crossflow microfiltration of oil-in-water emulsion using shear-induced diffusion; CFD and experimental studies, Desalination 357 (2015) 225–232.

[3] Y. Yang, R. Chen, W. Xing, Integration of ceramic membrane microfiltration with powdered activated carbon for advanced treatment of oil-in-water emulsion, Sep. Purif. Technol. 76 (2011) 373–377.

[4] H. Lotfiyan, F. Zokaee Ashtiani, A. Fouladitajar, S.B. Armand, Computational fluid dynamics modeling and experimental studies of oil-in-water emulsion microfiltration in a flat sheet membrane using Eulerian approach, J. Membr. Sci. 472 (2014) 1–9.

[5] T. Mohammadi, A. Esmaeelifar, Wastewater treatment of a vegetable oil factory by a hybrid ultrafiltration-activated carbon process, J. Membr. Sci. 254 (2005) 129–137.

[6] M. Zare, F. Zokaee Ashtiani, A. Fouladitajar, CFD modeling and simulation of concentration polarization in microfiltration of oil–water emulsions; Application of an Eulerian multiphase model, Desalination 324 (2013) 37–47.

[7] N. Javadi, F. Zokaee Ashtiani, A. Fouladitajar, A. Moosavi Zenooz, Experimental studies and statistical analysis of membrane fouling behavior and performance in microfiltration of microalgae by a gas sparging assisted process, Bioresour. Technol. 162 (2014) 350–357.

[8] S. Kasemset, A. Lee, D.J. Miller, B.D. Freeman, M.M. Sharma, Effect of polydopamine deposition conditions on fouling resistance, physical properties, and permeation properties of reverse osmosis membranes in oil/water separation, J. Membr. Sci. 425–426 (2013) 208–216.

[9] G. Liu, W. Wei, H. Wu, X. Dong, M. Jiang, W. Jin, Pervaporation performance of PDMS/ceramic composite membrane in acetone butanol ethanol (ABE) fermentation–PV coupled process, J. Membr. Sci. 373 (2011) 121–129.

[10] G.N. Vatai, D.M. Krstic, W. Höflinger, A.K. Koris, M.N. Tekic, Combining air sparging and the use of a static mixer in cross-flow ultrafiltration of oil/water emulsion, Desalination 204 (2007) 255–264.

[11] N. Moulai-Mostefa, O. Akoum, M. Nedjihoui, L. Ding, M. Jaffrin, Comparison between rotating disk and vibratory membranes in the ultrafiltration of oil-in-water emulsions, Desalination 206 (2007) 494–498.

[12] K. Scott, R. Jachuck, D. Hall, Crossflow microfiltration of water-in-oil emulsions using corrugated membranes, Sep. Purif. Technol. 22–23 (2001) 431–441.

[13] J.-P. Kim, J.-J. Kim, B.-R. Min, K.Y. Chung, J.-H. Ryu, Effect of glass ball insertion on vortex-flow microfiltration of oil-in-water emulsion, Desalination 143 (2002) 159–172.

[14] Z. Cui, S. Chang, A. Fane, The use of gas bubbling to enhance membrane processes, J. Membr. Sci. 221 (2003) 1–35.

[15] G. Ducom, H. Matamoros, C. Cabassud, Air sparging for flux enhancement in nanofiltration membranes: application to O/W stabilised and non-stabilised emulsions, J. Membr. Sci. 204 (2002) 221–236.

[16] A. Fouladitajar, F. Zokaee Ashtiani, H. Rezaei, A. Haghmoradi, A. Kargari, Gas sparging to enhance permeate flux and reduce fouling resistances in cross flow microfiltration, J. Ind. Eng. Chem. 20 (2014) 624–632.

[17] M. Khayet, C. Cojocaru, M. Essalhi, Artificial neural network modeling and response surface methodology of desalination by reverse osmosis, J. Membr. Sci. 368 (2011) 202–214.

[18] Q.-F. Liu, S.-H. Kim, Evaluation of membrane fouling models based on bench-scale experiments: a comparison between constant flowrate blocking laws and artificial neural network (ANNs) model, J. Membr. Sci. 310 (2008) 393–401.

[19] K.-J. Hwang, C.-Y. Liao, K.-L. Tung, Analysis of particle fouling during microfiltration by use of blocking models, J. Membr. Sci. 287 (2007) 287–293.

[20] A. Shahsavand, M.P. Chenar, Neural networks modeling of hollow fiber membrane processes, J. Membr. Sci. 297 (2007) 59–73.

[21] A. Fouladitajar, F. Zokaee Ashtiani, A. Okhovat, B. Dabir, Membrane fouling in microfiltration of oil-in-water emulsions; a comparison between constant pressure blocking laws and genetic programming (GP) model, Journal of Membrane Science Desalination (2013) 41–49.

[22] T.-M. Lee, H. Oh, Y.-K. Choung, S. Oh, M. Jeon, J.H. Kim, S.H. Nam, S. Lee, Prediction of membrane fouling in the pilot-scale microfiltration system using genetic programming, Desalination 247 (2009) 285–294.
[23] A. Nazari, S. Riahi, Computer-aided prediction of the ZrO_2 nanoparticles' effects on tensile strength and percentage of water absorption of concrete specimens, J. Mater. Sci. Technol. 28 (2012) 83–96.
[24] M. Rafiei Karahroudi, S. Mousavi Shirazi, K. Sepanloo, Optimization of designing the core fuel loading pattern in a VVER-1000 nuclear power reactor using the genetic algorithm, Ann. Nucl. Eng. 57 (2013) 142–150.
[25] H. Shokrkar, A. Salahi, N. Kasiri, T. Mohammadi, Prediction of permeation flux decline during MF of oily wastewater using genetic programming, Chem. Eng. Res. Des. 90 (2012) 846–853.
[26] A. Okhovat, S.M. Mousavi, Modeling of arsenic, chromium and cadmium removal by nanofiltration process using genetic programming, Appl. Soft Comput. 12 (2012) 793–799.
[27] C. Suh, B. Choi, S. Lee, D. Kim, J. Cho, Application of genetic programming to develop the model for estimating membrane damage in the membrane integrity test using fluorescent nanoparticle, Desalination 281 (2011) 80–87.
[28] A. Fouladitajar, F.Z. Ashtiani, B. Dabir, H. Rezaei, B. Valizadeh, Response surface methodology for the modeling and optimization of oil-in-water emulsion separation using gas sparging assisted microfiltration, Environ. Sci. Pollut. Res. 22 (2014) 2311–2327.
[29] J.R. Koza, Genetic Programming: On the Programming of Computers by Means of Natural Selection, MIT press, 1992
[30] J. Aguilar, G. González, Data Extrapolation Using Genetic Programming to Matrices Singular Values Estimation, in: Evolutionary Computation, 2006. CEC 2006. IEEE Congress on, IEEE, 2006, pp. 3227–3230, doi: 10.1109/CEC.2006.1688718.
[31] M. Khayet, C. Cojocaru, Artificial neural network model for desalination by sweeping gas membrane distillation, Desalination 308 (2013) 102–110.

Appendix 1

Table A1
Gas sparging experimental data used for GP modeling

Test number	Q_G (L/min)	C_{oil} (mg/L)	P (bar)	Q_L (L/min)	Permeate flux (Lm^2/h)	Rejection (%)
1	0.75	10,000	2	3	89.8	79.9
2	0.25	10,000	2	3	74.2	83.2
3	0.75	1,000	2	3	170.34	70.3
4	0.25	1,000	2	3	146.72	66.4
5	0.75	10,000	1	3	63.12	93.2
6	0.25	10,000	1	3	52.73	91.1
7	0.75	1,000	1	3	96.34	85.3
8	0.25	1,000	1	3	82.65	87.4
9	0.75	10,000	2	1	83.54	82.3
10	0.25	10,000	2	1	68.37	81.9
11	0.75	1,000	2	1	160.86	67.8
12	0.25	1,000	2	1	140.01	70.2
13	0.75	10,000	1	1	58.24	90.2
14	0.25	10,000	1	1	48.53	89.3
15	0.75	1,000	1	1	94.28	85.3
16	0.25	1,000	1	1	80.12	83.2
17	0.8	5,500	1.5	2	55.83	92.1
18	0.2	5,500	1.5	2	42	90.7
19	0.5	10,900	1.5	2	51.23	88.9
20	0.5	100	1.5	2	120.13	78.4
21	0.5	5,500	2.1	2	105.21	74.1
22	0.5	5,500	0.9	2	50.02	88.5
23	0.5	5,500	1.5	3.2	53.99	90.6
24	0.5	5,500	1.5	0.8	43.14	91.1
25	0.5	5,500	1.5	2	48.9	93.2
26	0.5	5,500	1.5	2	51.43	91.5
27	0.5	5,500	1.5	2	50.32	93.3

(*Continued*)

Table A1 (*Continued*)

Test number	Q_G (L/min)	C_{oil} (mg/L)	P (bar)	Q_L (L/min)	Permeate flux (Lm^2/h)	Rejection (%)
28	0.5	5,500	1.5	2	50.83	93.8
29	0.5	5,500	1.5	2	51.53	92.4
30	2	10,000	2	3	91.01	81.6
31	1	10,000	2	3	89.96	84.7
32	2	1,000	2	3	174.22	68.6
33	1	1,000	2	3	172.06	67.3
34	2	10,000	1	3	66.88	95.1
35	1	10,000	1	3	65.73	90.2
36	2	1,000	1	3	100.43	86.6
37	1	1,000	1	3	99.74	87.2
38	2	10,000	2	1	84.85	84.4
39	1	10,000	2	1	85.03	82.5
40	2	1,000	2	1	165.11	66.9
41	1	1,000	2	1	165.89	68.3
42	2	10,000	1	1	59.43	88.9
43	1	10,000	1	1	58.35	89.3
44	2	1,000	1	1	95.23	85.9
45	1	1,000	1	1	92.43	82.2
46	2.1	5,500	1.5	2	59.66	93.5
47	0.9	5,500	1.5	2	57.95	92.5
48	1.5	10,900	1.5	2	56.11	90.3
49	1.5	100	1.5	2	128.23	76
50	1.5	5,500	2.1	2	121.23	79.3
51	1.5	5,500	0.9	2	60.73	90.6
52	1.5	5,500	1.5	3.2	61.27	92
53	1.5	5,500	1.5	0.8	56.88	91.9
54	1.5	5,500	1.5	2	60.52	92.3
55	1.5	5,500	1.5	2	59.23	93
56	1.5	5,500	1.5	2	58.87	94.4
57	1.5	5,500	1.5	2	59.09	94.7
58	1.5	5,500	1.5	2	58.73	92.9
59	0.2	100	0.9	0.8	42	66.4
60	2.1	10,900	2.1	3.2	174.22	95.1